Damping and dispersion of linear longitudinal oscillations in a multi-component plasma

DOI:
10.1016/0378-4363(76)90049-8

Document status and date:
Published: 01/01/1976

Document Version:
Publisher's PDF, also known as Version of Record (includes final page, issue and volume numbers)

Physica 84C (1976) 394–400

DAMPING AND DISPERSION OF LINEAR LONGITUDINAL OSCILLATIONS IN A MULTI-COMPONENT PLASMA

A. J. D. LAMBERT, F. W. SLUIJTER and D. C. SCHRAM
Department of Applied Physics, Technische Hogeschool Eindhoven, Eindhoven, The Netherlands

Received 26 July 1976

This paper discusses linear dispersion and damping phenomena in multi-component Vlasov–Poisson plasma's without drift. The contamination damping is evaluated. The influence of temperature ratio, composition and mass ratio is discussed.

1. Introduction

Some years ago Fried and Gould published a by now classic paper on the dispersion of longitudinal waves in a hot uniform isotropic infinite plasma [1]. More recently their treatment was extended to account for the presence of more than one ion species [2]. Specifically the influence of the presence of a relatively small fraction of light ions in a plasma mainly consisting of heavier ions was investigated. Experimentally it was known that a small fraction of light ions may have a rather dramatic effect on the Landau damping, the so-called contamination damping [3]. This phenomenon provides us with a method that allows a relatively easy variation of parameters. This may be useful in experiments on current-driven turbulence. Usually the current-driven turbulence is interpreted in terms of linear theory, which implies the existence of definite modes.

In order to come to a better interpretation of these experiments, we intend to extend the existing linear theory with a strong emphasis on quantitative results especially concerning the role of such parameters as temperature ratio, ion-mass ratio and concentration ratio. As an important result we found that the contamination damping due to the light ions can be made to disappear if one has a sufficiently high temperature ratio between the electrons and the ions. The influence of the driving current is not treated here but is a subject of further study.

2. The Landau initial value problem

The well-known outcome of the Landau initial value problem leads to a kind of dispersion relation:

$$\epsilon^+(\hat{k}, \omega) = 1 - \sum_s \frac{\omega_{ps}}{\hat{k}} \int \frac{\mathrm{d}v \, \mathrm{d}F_s/\mathrm{d}v}{\hat{k}v - \omega_+} = 0. \tag{1}$$

The symbols have their usual meaning, and $\hat{k}$ is the wave-number. The subscript s refers to the different species of charged particles. The + index refers to the path of integration, to be taken such that $\epsilon^+(\hat{k}, \omega)$ is analytic in the upper half of the complex plane [4]. If the equilibrium velocity distribution is taken to be maxwellian:

$$F_s(v) = \frac{1}{\sqrt{2\pi} \cdot v_s} \exp\left[-\tfrac{1}{2}(v/v_s)^2\right], \tag{2}$$

then eq. (1) reads

$$2k^2 = \sum_s \theta_s \eta_s Z'(\zeta_s), \tag{3}$$

where k, θ_s, η_s and ζ_s are dimensionless quantities:

$$k = \hat{k}/K_e; \qquad \theta_s = T_s/T_e; \qquad \eta_s = n_s/n_e \tag{4}$$

$$\zeta_s = \frac{(\omega + \mathrm{i}\gamma)/k}{v_s\sqrt{2}} = \tilde{\omega}_s + \mathrm{i}\tilde{\gamma}_s, \tag{5}$$

in which K_e is the electron Debeye wave number, T the temperature, n the concentration. $\tilde{\omega}_s$ and $\tilde{\gamma}_s$ are real. The solution consists of different branches that will be indicated by index M. Quasi neutrality has been assumed.

$Z'(\zeta_s)$ is the derivative of the plasma dispersion function [5]. Numerical procedures are available to execute numerical calculations [6]. Approximate formulae are available too, the most well-known are based on the assumption

$$|\tilde{\gamma}| \ll |\tilde{\omega}|, \tag{6}$$

and on the series expansion

$$Z'(\zeta) \approx -\mathrm{i}\,\pi^{\frac{1}{2}}\,\tilde{\omega}\,\mathrm{e}^{-\tilde{\omega}^2} - 2 + 4\tilde{\omega}^2 + \ldots, \tag{7}$$

or the asymptotic expansion

$$Z'(\zeta) \approx -\mathrm{i}\,\pi^{\frac{1}{2}}\,\tilde{\omega}\,\mathrm{e}^{-\tilde{\omega}^2} + \tilde{\omega}^{-2} + \ldots. \tag{8}$$

Under assumption (6) the real and imaginary parts of eq. (3) decouple and this expression can be written in the following form, *cf.* for example, [7].

$$2k^2 = \sum_s \eta_s\,\theta_s\,\mathrm{Re}\,Z'(\tilde{\omega}_s), \tag{9}$$

$$\tilde{\gamma}e_M = 2\sqrt{\pi}\,\frac{\Sigma_s\,\eta_s\,\theta_s\,\tilde{\omega}_{s_M}\,\mathrm{e}^{-\tilde{\omega}^2_{sM}}}{\Sigma_s\eta_s\,\theta_s^{\frac{3}{2}}\,\delta_s^{\frac{1}{2}}\,\mathrm{d}/\mathrm{d}\tilde{\omega}_{s_M}\;\;\mathrm{Re}\,Z'(\tilde{\omega}_{s_M})}\,. \tag{10}$$

3. Solution for a single-component plasma

In these plasmas only one type of ion is present and the infinity of solutions of eq. (3) may be subdivided into two distinct groups: the electron- or high-frequency modes and the ionacoustic or low-frequency modes. The principal electron mode and the principal ion mode are the least damped ones. They are indicated by the indexes E and I, respectively.

The $\tilde{\omega}_s$ vs. $\tilde{\gamma}_s$ plots of these modes have basically the same shape if $\tilde{\omega}_{iE} \gtrsim 4$ and $\tilde{\omega}_{eI} \ll 1$ as is always true. The difference between both modes is most easily discussed by using the following concepts:

Initial phase velocity $\tilde{\omega}_{in}$ is the value of $\tilde{\omega}$ for $|k^2| \to 0$. For physically meaningful solutions in general: $\tilde{\omega} < \tilde{\omega}_{in}$.

Relevant domain is a rather arbitrarily chosen k-interval; we take $0 < k < 1$. Depending on the mode one considers and on θ ($= \theta_i$), this domain corresponds to a rather wide or narrow interval on the $\tilde{\omega}$-axis. The choice of the upper limit of the k-interval is connected with the plasma parameter.

Initial relative damping $(\tilde{\gamma}/\tilde{\omega})_{in}$ is the relative damping for $k \to 0$.

Initial acoustic velocity α_{in}; this concept only makes sense for the ion modes. It is the phase velocity for $k \to 0$.

For electron plasma oscillations, eq. (9) reads

$$2k^2 \approx Z'(\tilde{\omega}_e) + (1/\delta\,\tilde{\omega}_e^2), \tag{11}$$

$$(2/\theta)(k^2 + 1) \approx Z'(\tilde{\omega}). \tag{12}$$

The relevant domain for the electron mode follows from eqs. (11) and (8) by introducing the boundaries of the k-interval. It follows that $\tilde{\omega}_{eE} \gtrsim 1/\sqrt{2}$. The asymptotic expansions are, however, not correct when $\tilde{\omega} \lesssim 4$, but an exact calculation gives a similar result. Landau damping is then already overwhelming. We omit the index i for ions.

For the ion mode the relevant domain is found to be

$$\tfrac{1}{2}\sqrt{\theta} \lesssim \tilde{\omega} \lesssim \sqrt{\tfrac{1}{2}\theta}, \quad \text{so } \tilde{\omega}_{in} = \sqrt{\tfrac{1}{2}\theta}. \tag{13}$$

Eq. (13) indicates that the relevant domain corresponds to a very narrow $\tilde{\omega}$-band. The asymptotic expressions used are correct for $\theta \gtrsim 30$. At lower values of θ only an exact calculation helps us out, but Landau damping increases and the mode becomes more and more unrealistic. For the electron modes the value of $(\tilde{\gamma}/\tilde{\omega})_{in}$ is exactly zero. For the ion modes we make use of eqs. (8) and (10); in eq. (10) only the ion contribution in the denominator has to be taken into account. One then finds

$$(\tilde{\gamma}/\tilde{\omega})_{in} \approx -(\tfrac{1}{8}\pi)^{\frac{1}{2}}\cdot(\delta^{-\frac{1}{2}} + \theta^{\frac{3}{2}}\,\mathrm{e}^{-\frac{1}{2}\theta}). \tag{14}$$

For $\theta \gtrsim 30$ the second term on the right, the ion contribution, may be neglected with respect to the electron contribution and the initial relative damping becomes θ-independant. For the relative damping as a function of $\tilde{\omega}$ we find

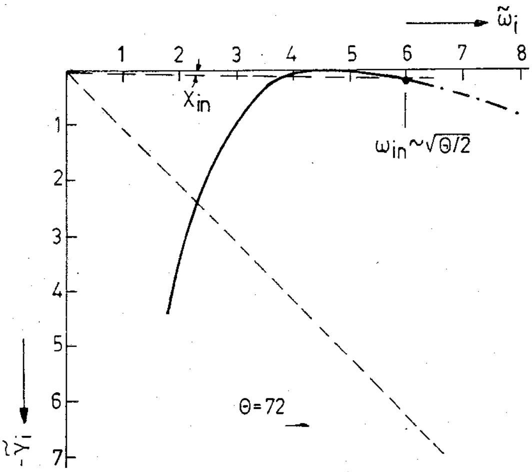

Fig. 1. $\tilde\omega$–$\tilde\gamma$ plot of the principal ion mode in a single-component plasma. $\tan \chi_{in} = (\tilde\gamma/\tilde\omega)_{in}$, $\theta = 72$.

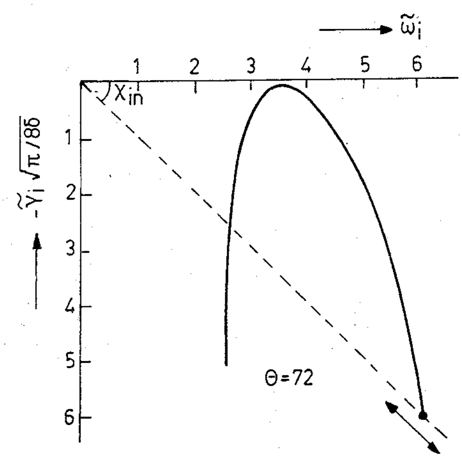

Fig. 2. The same $\tilde\omega$–$\tilde\gamma$ plot, the $\tilde\gamma_i$-scale being multiplied by $\sqrt{\pi/8\delta}$ for showing clearly the electron influence.

$$(\tilde\gamma/\tilde\omega) \approx -(\sqrt{\pi}/\theta^{\frac{3}{2}})\, \tilde\omega^{3}(\delta^{-\frac{1}{2}} + \theta^{\frac{3}{2}}\, e^{-\tilde\omega^2}). \tag{15}$$

Figs. 1 and 2 show the negative slope of the curve for $\tilde\omega$ in between 4 and $\tilde\omega_{in}$. The point where the damping is minimal depends only slightly on θ as is shown in table I.

Fig. 2 shows clearly that the physically relevant part of the $\tilde\omega$–$\tilde\gamma$ curve ends in an intersection point with a line through the original with a slope of $-(\pi/8\delta)^{\frac{1}{2}}$.

An interesting feature of the complex frequency locus in the parameter domain under consideration

Table I
$\tilde\omega$-value for which the electron and ion contribution to the Landau damping are equal (approximation of the maximum in fig. 2)

θ	$\tilde\omega$
10	2.67
100	3.27
1000	3.77
10000	4.20

will be discussed at the end of this section. The dimensionless real frequency $\bar\omega = \omega/\omega_{pi}$ follows from

$$\bar\omega = \tilde\omega k\sqrt{2/\theta}. \tag{16}$$

In the case $\tilde\omega \gtrsim 4$ it follows from eqs. (8) and (12):

$$\bar\omega^2 \approx k^2/(1+k^2) \tag{17}$$

and hence $\tilde\omega^2 = \frac{1}{2}\theta\,(1-\bar\omega^2)$. (18)

Eq. (15) may be written as:

$$\frac{\tilde\gamma}{\tilde\omega} = \frac{\bar\gamma}{\bar\omega} \sim -\tfrac{1}{8}\pi\,(1-\bar\omega^2)^{\frac{3}{2}}\,(\delta^{-\frac{1}{2}} + \theta^{\frac{3}{2}}\, e^{-\frac{1}{2}\theta(1-\bar\omega^2)}), \tag{19}$$

which is equal to zero for $\bar\omega = 1$.

We have, however, used approximate formulae. For high θ-values, numerical calculation shows that the maximum nearly touches the real axis (fig. 3). The initial slope in fig. 3 is found from eq. (15) with $\tilde\omega = \tilde\omega_{in}$. For high θ, eq. (14) may be used.

When θ decreases below $\theta \lesssim 30$ the initial slope χ rises sharply. Consequently the maximum in the curve disappears: the ions make themselves felt strongly in the damping process.

4. Solution of the dispersion relation for a multi-component plasma

The electron branch is not essentially affected by the presence of more than one type of ion, and therefore we ignore it. In the ion branch, however, quantitative changes occur. In the dispersion relation (9) two ion terms are present that may be of the same order of magnitude within a certain parameter domain.

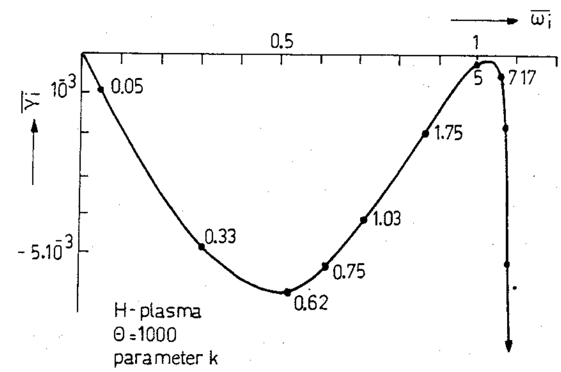

Fig. 3. $\tilde{\omega}_i - \tilde{\gamma}_i$ plot of a single component plasma with high θ-value shows a sharp maximum at $\tilde{\omega} \approx 1$. The origin is related to the $\tilde{\omega}_i = \tilde{\omega}_{in}$ point of the $\tilde{\omega}$–$\tilde{\gamma}$ plot. The damping is almost completely due to electrons.

For simplicity we restrict ourselves again to single-charged ions of equal temperature which give rise to the appearance of two more parameters:

$$\text{mass ratio: } \mu = m_2/m_1, \tag{20}$$

$$\text{dimensionless density: } \eta = n_1/n_e. \tag{21}$$

By convention: $m_2 > m_1$. Indexes 1 and 2 represent the ion species. Then the equivalent of eq. (12) reads:

$$(2/\theta)(k^2+1) = \eta Z'(\tilde{\omega}_1) + (1-\eta) Z'(\tilde{\omega}_2), \tag{22}$$

with

$$\tilde{\omega}_2 = \tilde{\omega}_1 \sqrt{\mu}, \tag{23}$$

and the restriction

$$|\tilde{\gamma}| \ll |\tilde{\omega}|. \tag{24}$$

Relation (12) was first investigated by Fried *et al.* [2].

4.1. The generalized light-ion mode

We assume $\tilde{\omega}_2 \gtrsim 4$, in combination with eq. (24) eq. (22) reduces to

$$\frac{2}{\theta}(k^2+1) = \eta Z'(\tilde{\omega}_1) + \frac{1-\eta}{\mu}\frac{1}{\tilde{\omega}_1^2}. \tag{25}$$

If θ is chosen sufficiently high, there may be physically relevant solutions with $\tilde{\omega}_1 \gtrsim 4$ too, and eq. (25) becomes:

$$(2/\theta)(k^2+1) = M/\tilde{\omega}_1^2, \tag{26}$$

where M, the mixing factor, is defined as

$$M = \eta + \frac{1-\eta}{\mu}, \quad \text{thus } \mu^{-1} \leqslant M \leqslant 1. \tag{27}$$

Instead of eq. (13), we read for the relevant domain

$$\tfrac{1}{2}\sqrt{\theta M} \lesssim \tilde{\omega}_1 \lesssim \sqrt{\tfrac{1}{2}(\theta M)}, \quad \text{thus } \tilde{\omega}_{in} = \sqrt{\tfrac{1}{2}(\theta M)} \tag{28}$$

and hence

$$\alpha_{in} = \sqrt{M}. \tag{29}$$

The additional condition for θ is

$$\theta \gtrsim 30/M. \tag{30}$$

In this case, the extension of eqs. (14) and (15) leads, respectively, to

$$\tilde{\gamma}/\tilde{\omega}_{in} \approx -(\tfrac{1}{8}\pi M)^{\frac{1}{2}} \{\delta^{-\frac{1}{2}} + \theta^{\frac{3}{2}}(\eta\, e^{\frac{1}{2}(-\theta M)} + (1-\eta)\sqrt{\mu}\, e^{\frac{1}{2}(-\mu\theta M)})\}, \tag{31}$$

and

$$\frac{\tilde{\gamma}}{\tilde{\omega}} \approx -\frac{\sqrt{\pi}}{\theta^{\frac{3}{2}} M}\tilde{\omega}^3 \{\delta^{-\frac{1}{2}} + \theta^{\frac{3}{2}}(\eta\, e^{-\tilde{\omega}^2} + (1-\eta)\sqrt{\mu}\, e^{-\mu\tilde{\omega}^2})\}, \tag{32}$$

and, if eq. (30) holds, the exponentials in eq. (31) can be ignored, the $\tilde{\omega}$–$\tilde{\gamma}$ plot behaves as in figs. 1 and 2. At increasing η the slope χ_{in} changes continuously between $(\pi/8\delta\mu)^{\frac{1}{2}}$ and $(\pi/8\delta)^{\frac{1}{2}}$, and the curve changes continuously between the heavy-ion plot and the light-ion plot.

4.2. Splitting up at lower θ-values

When we only restrict ourselves to $\theta \gtrsim 30$, $\tilde{\gamma}/\tilde{\omega}$ is easily calculated for the heavy-ion case. If η increases from zero to very small values, the exponential in eq. (31) will have a growing contribution to $(\tilde{\gamma}/\tilde{\omega})_{in}$,

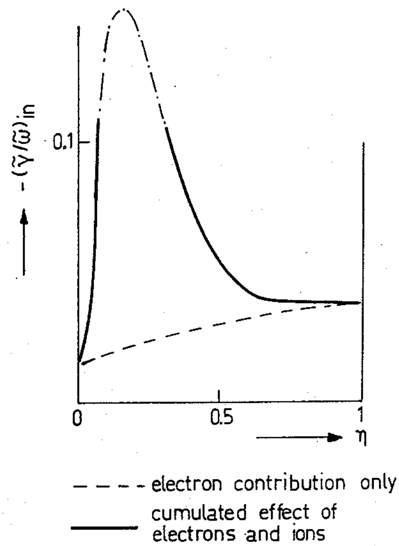

Fig. 4. Schematic plot of initial relative damping as a function of η in a two-component plasma at sufficiently high θ-values. If θ decreases the maximum value of $(\tilde{\gamma}/\tilde{\omega})_{in}$ increases and the curve splits into two separate branches (*cf.* fig. 5).

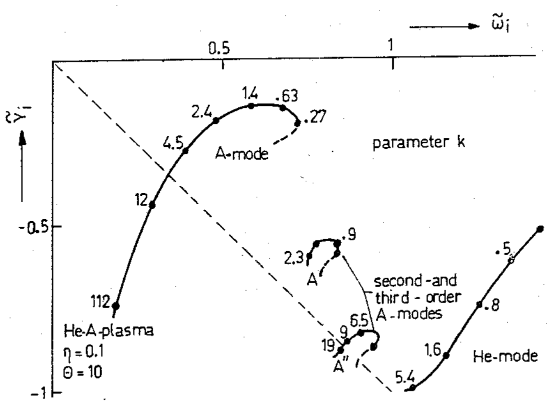

Fig. 5. Rupture of the $\tilde{\gamma}-\tilde{\omega}$ curve at a sufficiently low θ-value. Note that at higher θ-values the A-mode and the He-mode are connected to form the generalized light-ion mode. The black dots indicate $\tilde{\omega}-\tilde{\gamma}$ values for which $k^2 = 0$. Plot is calculated by using a numerical method on a digital computer.

because of the fact that the small η has not much influence on M. This contribution may be much more important than in the light-ion case: this is the so-called contamination damping. If η increases the initial damping will go through a maximum value but, at low θ, this maximum will be beyond the scope of eqs. (24) and (31). If η increases more and more, M increases too and the contribution of the exponentials diminishes. In fig. 4 the contribution of electrons and light ions to the initial relative damping is sketched. There may occur a splitting up in the heaviest damped η-interval, at sufficiently low θ values [2]. Of course a numerical solution is possible. Fig. 5 shows the $\tilde{\gamma}$ vs. $\tilde{\omega}$-plot for the case of an Ar/He-plasma, and the splitting up into two separate branches (in this case $\theta = 10$ and $\eta = 0.1$).

The rightmost branch is a (deformed) part of the modified light-ion branch, the other is a modified heavy-ion branch. At lower η values the light-ion branch evolves into a higher-order heavy-ion mode which is heavier damped. If one plots the two branches in one graph, each with its appropriate normalization, they would coincide approximately, the difference being due to the presence of the other type.

With the aid of a graphical method the behaviour can be easily understood. The $Z'(\zeta)$ plot has already for an infinitesimally small negative imaginary part of ζ an intersection point with the positive real Z'-axis [5]. In the expression

$$(1/\theta)\,Z'(\zeta_e) + \eta Z'(\zeta_1) + (1-\eta)Z'(\zeta_2) = 2k^2, \qquad (33)$$

we have to add three of those contributions. In the case of ion-acoustic modes, the electron term can safely be approximated by $-(2/\theta)$. Hence if $\eta = 0$; the plot of the left-hand side of eq. (33) is the same as that for $Z'(\zeta_2)$, but shifted to the left over a distance $2/\theta$. The small imaginary contribution of the electrons causes an additional, but small, shift downward. That means (fig. 6) that a finite amount of damping is needed for the appearance of one or two intersection points with the real Z'-axis. A physically relevant solution is represented by an intersection point to the right of 0' in fig. 6. At low θ values a lot of damping is required.

If we allow a small η then the influence of the light ions is almost entirely determined by the light ion contribution. The expression $\eta Z'(\zeta_1) + (1-\eta)Z'(\zeta_2)$ differs from $Z'(\zeta_2)$ by a deformation that is visualized schematically in fig. 7. The position of this deformation is mainly determined by μ and its importance by η. Fig. 6 gives some exact results that make plots like fig. 5 plausible.

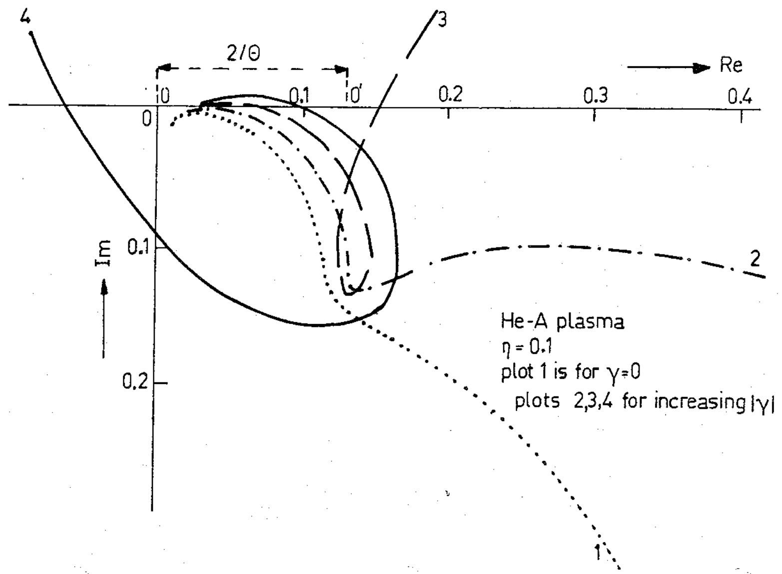

Fig. 6. The behaviour of $[Z'(\zeta_e)/\theta] + \eta Z'(\zeta_1) + (1-\eta)Z'(\zeta_e)$ for $\tilde{\omega}_1 \gtrsim 1$ and $\tilde{\omega}_e \ll 1$, $\mu = 10$ (A/He plasma), $\eta = 0.1$. A certain value of θ is represented by translation of the origin over a distance $2/\theta$ to the right along the Re-axis. The distance between intersection points of the curves with the Re-axis and the origin represents the value of $k^2/2\theta$. An intersection point on the negative Re-axis represents an imaginary k-value and is of no physical interest.

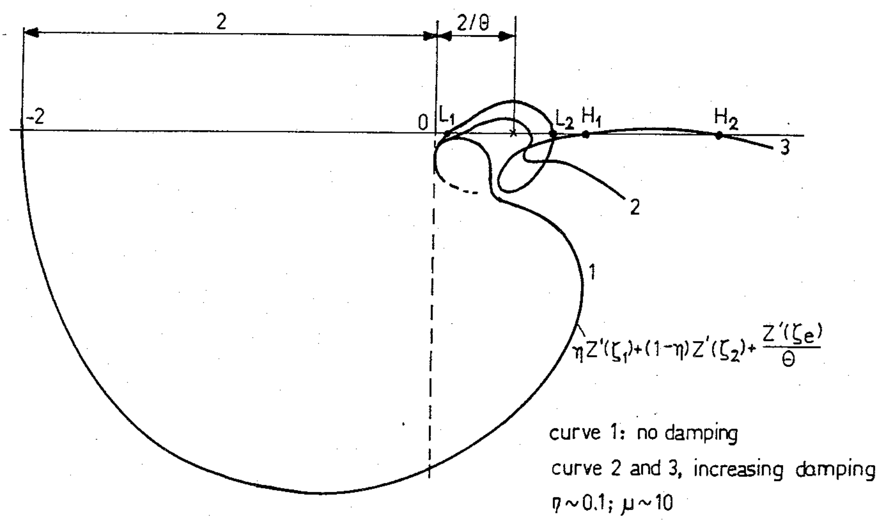

Fig. 7. Behaviour of different intersection points. The points L_1 and L_2 represent the generalized light-ion-modes. If θ is sufficiently low, the intersection-points H_1 and H_2 appear first, when the damping increases from zero, on the positive real axis. Thus in this case the heavy-ion mode is less damped than the generalized light-ion mode. The appearance of a pair of intersection-points on the positive real axis represents the "bending down" as demonstrated in figs. 1, 2 and 5.

5. Conclusion

A detailed study of the dispersion relation of multi-component plasmas shows that a small fraction of light ions gives rise to strongly enhanced damping if the ratio θ between the temperatures of electrons and ions within a certain interval. This range is typically between $5 \lesssim \theta \lesssim 100$, which happens to be usual gas-discharge and ohmic-heated plasma parameter range. This means that the contamination damping can indeed be used as a sensitive tool to check the applicability of linear concepts for nonlinear ion-acoustic plasma phenomena.

At increasing θ-values the contamination damping diminishes. At low θ-values the damping at $\eta = 0$ (no light ions) is already overwhelming and the contamination damping has no physical significance.

The width of the above meant θ-interval depends on both the mass ratio μ and the light-ion concentration. The maximum value of the contamination damping is found at $\eta \sim \mu^{-1}$.

Discussion of the contamination damping is possible with the aid of fig. 7. Curve 1 shows a dent which moves clockwise with increasing η; its depth becomes more and more pronounced with increasing μ. A clockwise displacement of the dent is related to an increasing damping of the heavy-ion mode, and a decreasing damping of the light-ion mode. If one starts out with a parameter choice such that both the light- and heavy-ion modes are weakly damped, a decreasing θ-value makes the light-ion mode increasingly damped. At a fixed k-value the heavy-ion mode will become heavier damped if θ increases.

References

[1] B. D. Fried and R. W. Gould, Phys. Fluids 4 (1961) 139.
[2] B. D. Fried, R. B. White and T. K. Samec, Phys. Fluids 14 (1971) 2388.
[3] I. Alexeff, W. D. Jones and D. Montgomery, Phys. Rev. Lett. 19 (1967) 422.
[4] R. W. B. Best, Physica 64 (1973) 387.
[5] B. D. Fried and R. W. Gould, The Plasma Dispersion Function (Academic Press, New York, 1961).
[6] W. Gautschi, Commun. ACM 12 (1969) 635.
[7] D. C. Montgomery, Theory of the Unmagnetized Plasma (Gordon and Breach, New York, 1971).